ABSTRACT

A motor case for an air-launched missile was analyzed using MSC/NASTRAN's SOL 64. The shell was thickened at the top for support purposes and caused large positive radial deformations to occur at the top and bottom and negative radial deformations to occur at the sides when burst pressures were applied. The non-circular shape of the motor case cross section had a significant influence on the stiffness of the structure which exhibited geometric non-linear behavior. Several NASTRAN models, including a solid element model and several plate element models, were used to analyzed the motor case.

INTRODUCTION

Vought Corporation is currently designing an air launched missile which attaches to an aircraft at the pylon attach hooks at the positions shown in Figure 1. The aft pylon attach hook is an integral part of the solid rocket motor case shown in Figure 2. Section A-A, shown in Figure 2, is a cross section of the motor case at the pylon attach point and shows that the inside radius of the motor case, and consequently, the shell thickness varies. When analyzed with a burst pressure loading condition, some interesting results were observed. The purpose of this paper is to present the results and to offer explanations for the behavior.

NASTRAN SOLID ELEMENT MATH MODEL OF MOTOR CASE

The motor case was initially modeled with 8 noded solid elements as shown in Figure 3. Two planes of symmetry were assumed and the appropriate boundary conditions were imposed. The edge of the model with the thick section is the plane of symmetry in the longitudinal direction and the plane dividing the circumferential halves is the second plane of symmetry. The thickest part of the shell was 2.05 inches at the intersection of the two planes of symmetry and tapered to 0.50 inches in the circumferential direction. The shell thickness also tapered to 0.336 inches in the longitudinal direction at the free end. Although the shell thickness varied, the outside radius of the motor case was 11.0 inches throughout. The model was supported to reflect the proper boundary conditions and an additional support in the vertical direction was used to maintain numerical stability.

DEFORMATION COMPUTED BY CLASSICAL FORMULA

The in-flight load condition of the motor case was represented with a 2000 psi burst pressure load and longitudinal forces applied at the free end to simulate a capped end effect. The classical formula for computing the radial

deformation of a pressure vessel does not apply in the case of a shell with varying thickness, but for comparison purposes, the radial deformation of a 0.50 inch thick, 10.75 inch radius pressure vessel with a 2000 psi burst pressure load is computed below:

$$R = 10.75"$$

$$t = 0.50"$$

$$E = 10.5 \times 10^6 \text{ psi (Aluminum)}$$

$$\nu = 0.33 \text{ (Aluminum)}$$

$$q = 2000 \text{ psi}$$

$$\Delta R = \frac{q R^2}{E t} \left(1 - \frac{\nu}{2} \right)$$

$$= \frac{2000 (10.75)^2}{(10.5 \times 10^6) 0.50} \left(1 - \frac{0.33}{2} \right)$$

$$= 0.03676"$$

$$\Delta D = 2 \Delta R$$

$$= 0.07352$$

The radial deformations calculated above will serve as a baseline from which to compare the radial deformations given by the NASTRAN analysis.

DEFORMATIONS COMPUTED BY NASTRAN

MSC/NASTRAN's geometric non-linear solution sequence (SOL 64) was used for the analysis of the motor case math model. Figure 4 shows the normalized deformation of a typical grid point at each iteration as the solution converged. The static analysis (Subcase 1) yielded deformations that were as much as three times the deformation in the converged solution. Figure 4 shows that the solution was very close to the converged solution after four iterations.

Figure 5 shows the undeformed cross sectional shape overlayed by the deformed shaped at both ends of the solid element model. As shown, the motor case deflected radially outward at the top and bottom, but deflected radially inward at the sides. At the longitudinal plane of symmetry, the combined deformation at the top and bottom was 0.1522 inches or 2.07 times ΔD calculated by the classical formula. The largest negative radial deformation at the side was -0.05255 inches or -1.43 times ΔR. At the free end, which tapers to 0.336 inches, the combined radial deformation at the top and bottom was 0.2074 inches or 2.82 times ΔD and at the side, the largest negative radial deformation was -0.01497 inches or -0.407 times ΔR. Large radial deformations at the top and bottom and negative radial deformations at the sides was not the expected behavior considering the added thickness of the shell at the top and the burst pressure loading condition. Further study, however, revealed several possible explanations for the behavior.

DISCUSSION OF BEHAVIOR

One possible cause for the large radial deformations at the top and bottom and the negative radial deformations at the sides is the non-circular shape of the motor case cross sectional area. With regard to deformation, the most efficient way for a pressure vessel to resist a pressure load is by membrane forces. This means of resisting pressure becomes less efficient as the pressure vessel's cross section deviates from a circular shape. An extreme example of a non-circular shape would be a square section which would rely predominately on bending forces to resist the pressure. Figure 6 shows plots of the deformed shape of pressure vessels with both circular and square cross sections which had the same enclosed area, the same shell thickness, and the same material properties. Also, the deformations for both structures were plotted to the same scale. The deformation of the circular cross section is

not discernable at the plotted scale, but relatively large bending deformations of the square cross section are evident. For a pressure vessel which has a shape somewhere between circular and square, such as the motor case, there will be a combination of bending and membrane forces to resist the pressure. It was the deformation due to the bending which caused the large deflection at the top and bottom and the inward deflections at the sides of the motor case. Simply stated, the motor case tended to take the most efficient cross sectional shape (circular) when the pressure load was applied.

The non-circular shape of the pressurized surface area may also be a factor which caused the large radial deformations at the top and bottom. Because of the "oval" shape of the pressurized surface area, the vertical direction had a larger component of the applied load than the horizontal direction and therefore should have resulted in a larger vertical deformation. This theory was tested by applying a negative 2000 psi pressure to the circular outside surface of the solid element model. The results, however, were about the same as the analysis where the loads were applied to the inside surface. This shows that the applied load vector had little effect on the deformed shape of the motor case.

Another possible contribution to the deformed shape of the motor case may be the bending introduced by the eccentric loads acting at the "thick" section. The longitudinal forces are applied at the free end of the model where the shell thickness is 0.336 inches. Where the motor case tapers to a larger thickness, the neutral axis of the section is no longer in line with the force. The eccentricity of the force introduces bending in the structure and could account for part of the large deformation at the top of the motor case. Figure 7, which is a NASTRAN plot of the deformed shape of an eccentrically loaded beam, illustrates this concept.

NASTRAN PLATE ELEMENT MATH MODELS OF MOTOR CASE

The ideas presented in the previous paragraphs were studied further with several NASTRAN models using CQUAD4 plate elements. Initially, a model was created which had a uniform shell thickness of 0.50 inches and had a radius of 10.75 inches. a run was made with the 2000 psi pressure load and resulted in a uniform radial deformation of 0.03642 inches which is very close to the calculated value of 0.03676 inches. This run provided confidence that the modeling techniques were correct.

Shown in Figure 8 is a plate element model of the motor case in which the elements are located at the mid-shell thickness of the motor case. The deformed shape of the model is shown in Figure 9 and shows that the same deformed shape was observed for both the plate element model and the solid element model. At the plane of symmetry, the combined deformation at the top and bottom was 0.1543 inches or 2.10 ΔD and the maximum radial deformation at the side was -0.0370 or -1.01 ΔR. At the free end, the combined deformation at the top and bottom was 0.2069 or 2.81 ΔD and the maximum radial deformation at the side was -0.0026 or -0.071 ΔR. These results compare very well with the results of the solid element model analysis.

Another plate element model shown in Figure 10 was created to eliminate the effects of the non-circular shape of the motor case cross section and to eliminate the effects of the eccentric longitudinal loads. A radial coordinate of 10.75 inches was used for all geometric grid points and all other data including the varying thickness was kept the same as the variable radial geometry plate model (see Figure 8). Plots of the deformed shape are shown in Figure 11 and show that the negative radial deformations were eliminated. At the plane of symmetry, the combined radial deformation at the top and bottom was 0.05741 inches or 0.781 ΔD and the minimum radial deformation at the side was 0.01716 inches or 0.467 ΔR. At the free end, the

combined radial deformation at the top and bottom was 0.1279 inches or 1.74 ΔD and the radial deformation at the side was 0.0435 or 1.18 ΔR. The analysis showed that the geometric shape of motor case cross section did have a significant effect on the deformed shape. Also, the magnitude of the deformations were significantly less and the variation of the radial deformations were due totally to the varying thickness of the shell.

The effects on the deformation due to the non-circular cross sectional shape and the eccentric longitudinal loads were isolated by applying the 2000 psi pressure load and the longitudinal forces separately. The plate element model with the varying radial geometry and the varying thickness (see Figure 8) was used for this analysis. Figures 12 and 13 show the deformed shape of the motor case for the pressure only load case and the longitudinal only load case, respectively. At the plane of symmetry, the combined radial deformation at the top and bottom was 0.1669 inches or 2.27 ΔD for the pressure only load case and was -0.0067 inches or -0.091 ΔD for the longitudinal only load case. This shows that the eccentricity of the longitudinal forces had very little influence on the vertical deformation of the motor case. At the side, the radial deformation was -0.03313 inches or -0.901 ΔR for the pressure only load case and was -0.0071 inches or -0.192 ΔR for the longitudinal only load case. This shows that about 18 percent of the negative radial deformation at the side was due to the longitudinal load. At the free end where the longitudinal loads were applied, the deformations at the top and bottom due to the longitudinal loads were not significant. These analyses show that most of the radial deformation of the motor case was due to the stiffness effects of the non-circular cross section of the motor case.

STRESS COMPUTATIONS

The theoretical stresses for a 0.50 inch thick pressure vessel with a radius of 10.75 inches and a 2000 psi pressure load are calculated below:

$$\sigma_1 = \frac{q\,R}{2\,t} = \text{longitudinal stress}$$

$$= \frac{2000\ (10.75)}{2\ (0.50)}$$

$$= 21{,}500 \text{ psi}$$

$$\sigma_2 = 2\ \sigma_1 = \text{hoop stress}$$

$$= 2\ (21{,}500)$$

$$= 43{,}000 \text{ psi}$$

These stress values will be used to compare with the NASTRAN computer stresses for the motor case.

A stress contour plot of the plate element model shown in Figure 14 shows that the highest major principal stresses occurred along the side of the motor case where the negative radial deformations were observed. The maximum stress near the longitudinal plane of symmetry was 49,849 psi or 1.16 times σ_2. The portions of membrane and bending stress were 81 percent and 19 percent, respectively, at this point. At the free end where the shell thickness tapers to 0.336 inches, the maximum stress was 65,152 psi or 1.52 times σ_2. The membrane and bending stresses accounted for 94 percent and 6 percent, respectively, of the total stress at this point. The total stress was higher at the free end because of the decreased shell thickness, but the percentage of bending stress was less because of the circular cross sectional shape at that point.

The solid element model had a stress distribution which was similar to that of the plate element model. The maximum stress near the longitudinal plane of symmetry was 54,231 psi or 1.26 σ_2 and the portions of membrane and bending stress were 75 percent and 25 percent, respectively. At the free end where the shell thickness tapers to 0.336 inches, the maximum stress was

66,146 psi or 1.54 σ_2. The stress breakdown was 91 percent membrane and 9 percent bending. The bending stresses of the solid element model were larger at the longitudinal plane of symmetry and therefore, resulted in a higher total stress at that point than was seen for the plate element model. Also, the bending stress at the free end was slightly higher for the solid element model and resulted in a slightly higher total stress.

CONCLUSIONS

Motor Case

1. The cross sectional shape of the motor case had a large influence on the structural stiffness of the motor case and resulted in large radial deformations at the top and bottom and negative radial deformations at the sides.
2. The longitudinal forces due to the capped end had little influence on the vertical deformation of the motor case. The eccentricity of the thick section was too small for this effect to have a significant influence. The longitudinal forces did make a significant contribution to the negative radial deformation at the side, however.
3. Because of the non-circular shape of the pressurized surface area, a larger component of the pressure load was applied in the vertical direction. This effect, however, did not contribute significantly to the deformation of the structure.

MSC/NASTRAN

1. The deformations of the solid element model and the plate element model were about the same.
2. The membrane stresses were similar for both the solid element model and the plate element model, but the bending stresses were greater in the solid element model. This resulted in greater total stresses for the solid element model at the high bending areas.

3. Non-circular shaped pressure vessels should be analyzed with a geometric non-linear solution sequence because the structural stiffness does change significantly as the structure deforms.
4. The cost of analyzing the plate element model was about 75 percent of the cost of analyzing the solid element model.

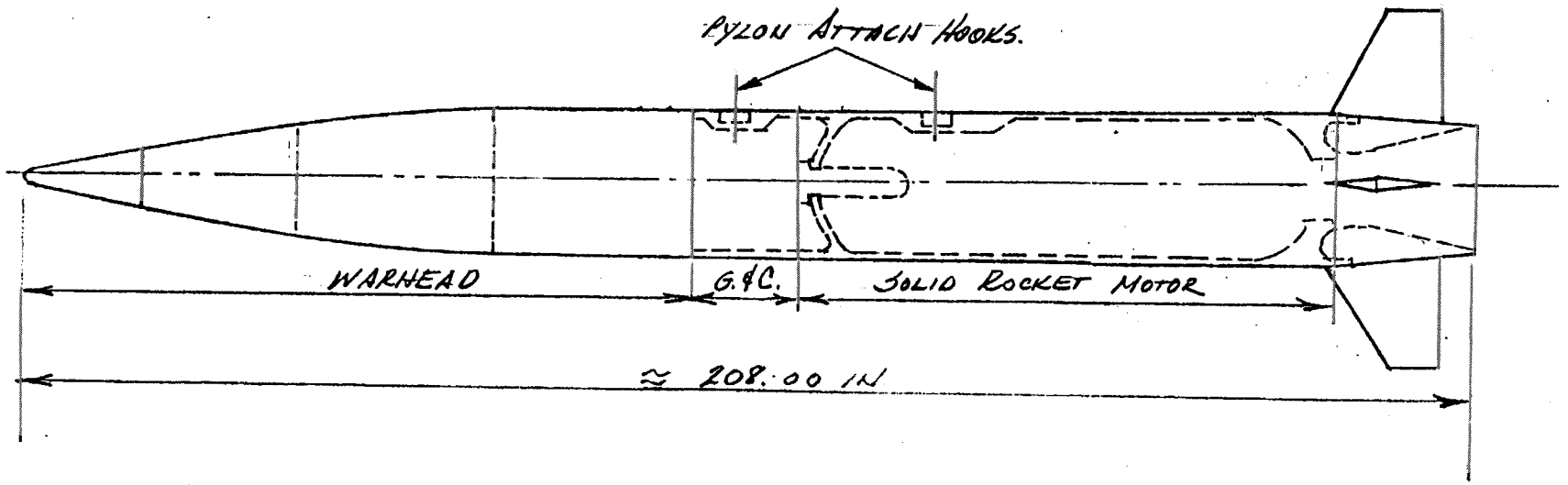

FIGURE 1. AIR-LAUNCHED MISSILE WITH SOLID ROCKET MOTOR

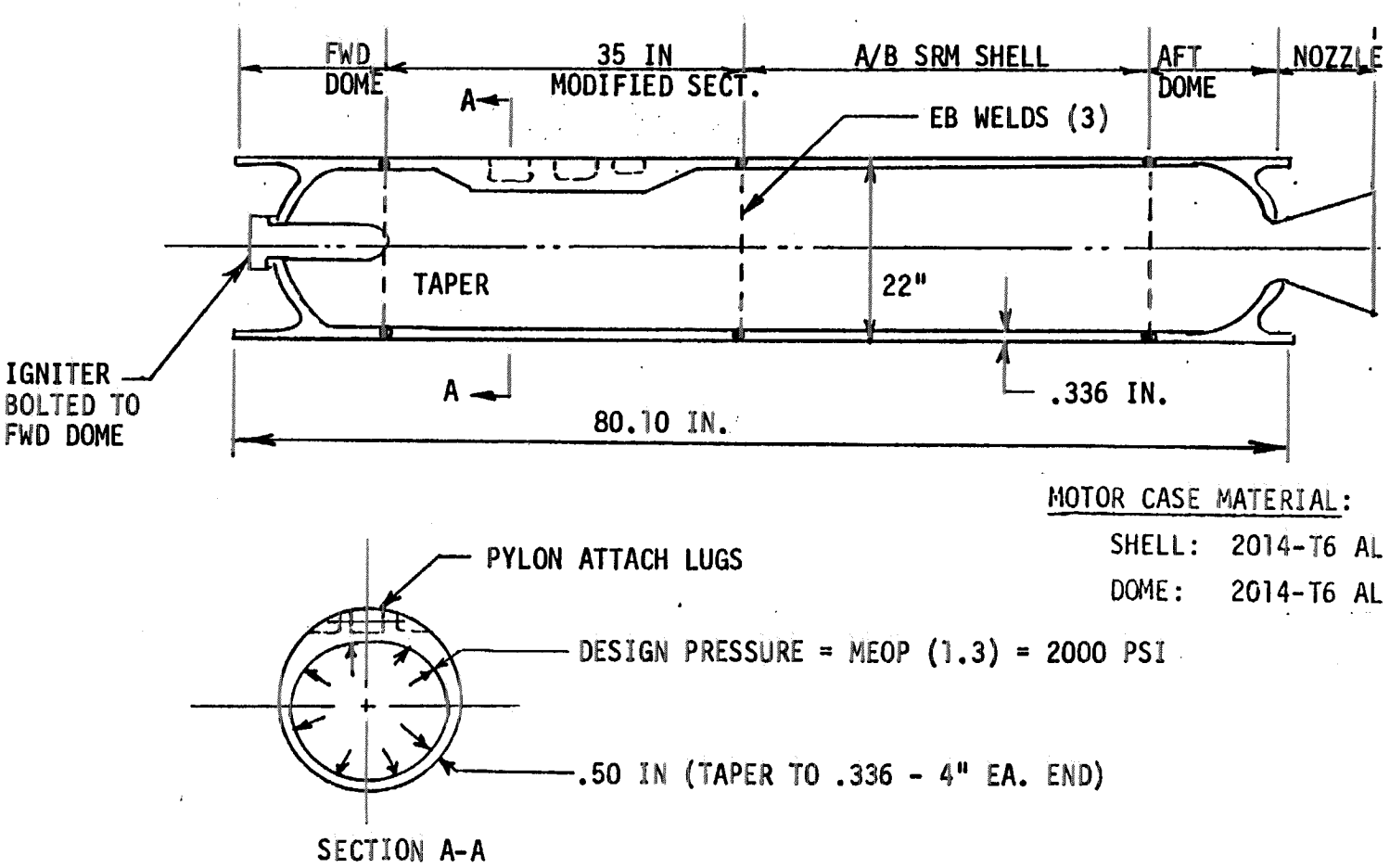

FIGURE 2. SOLID ROCKET MOTOR

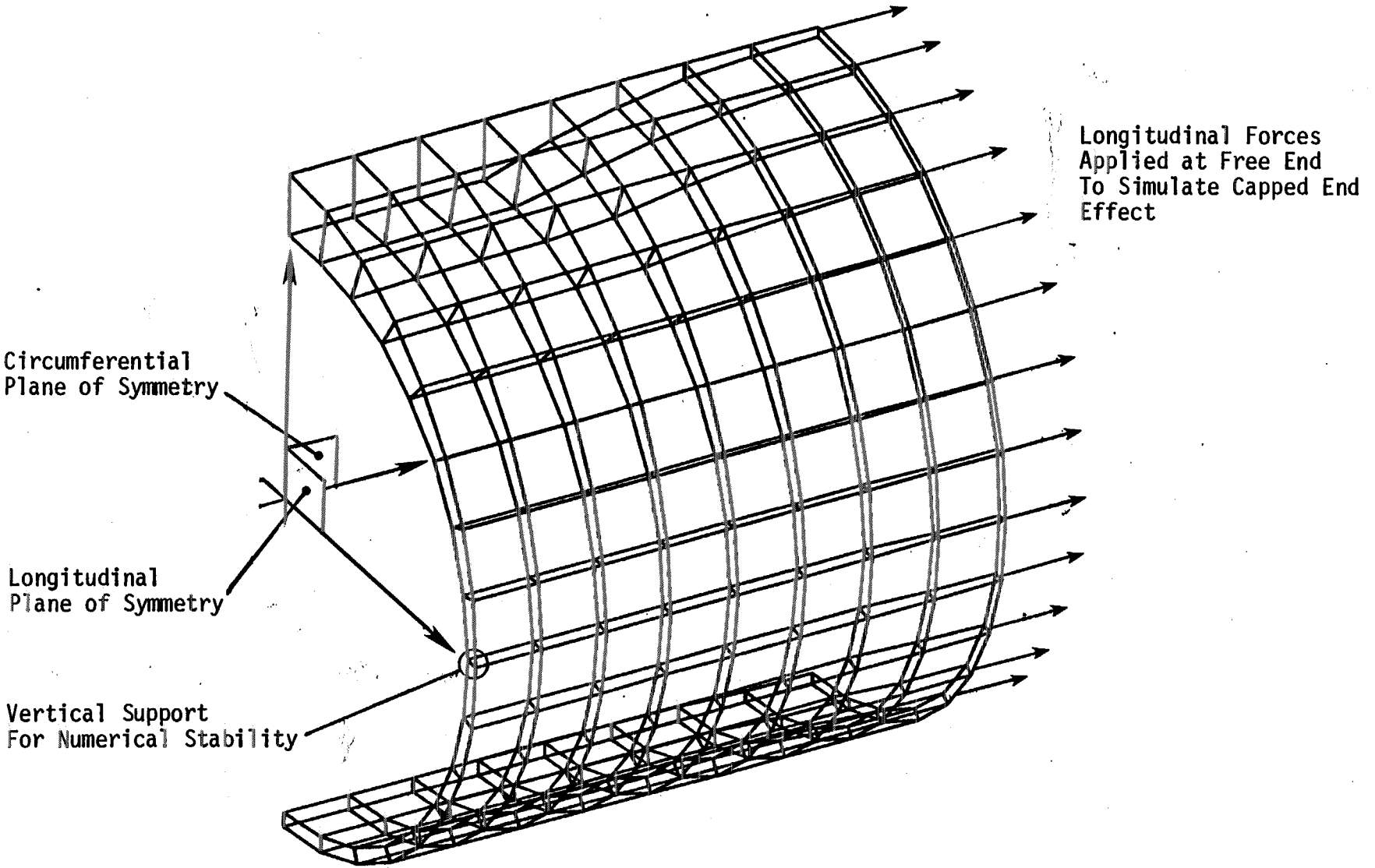

FIGURE 3. NASTRAN Solid Element Model of Motor Case

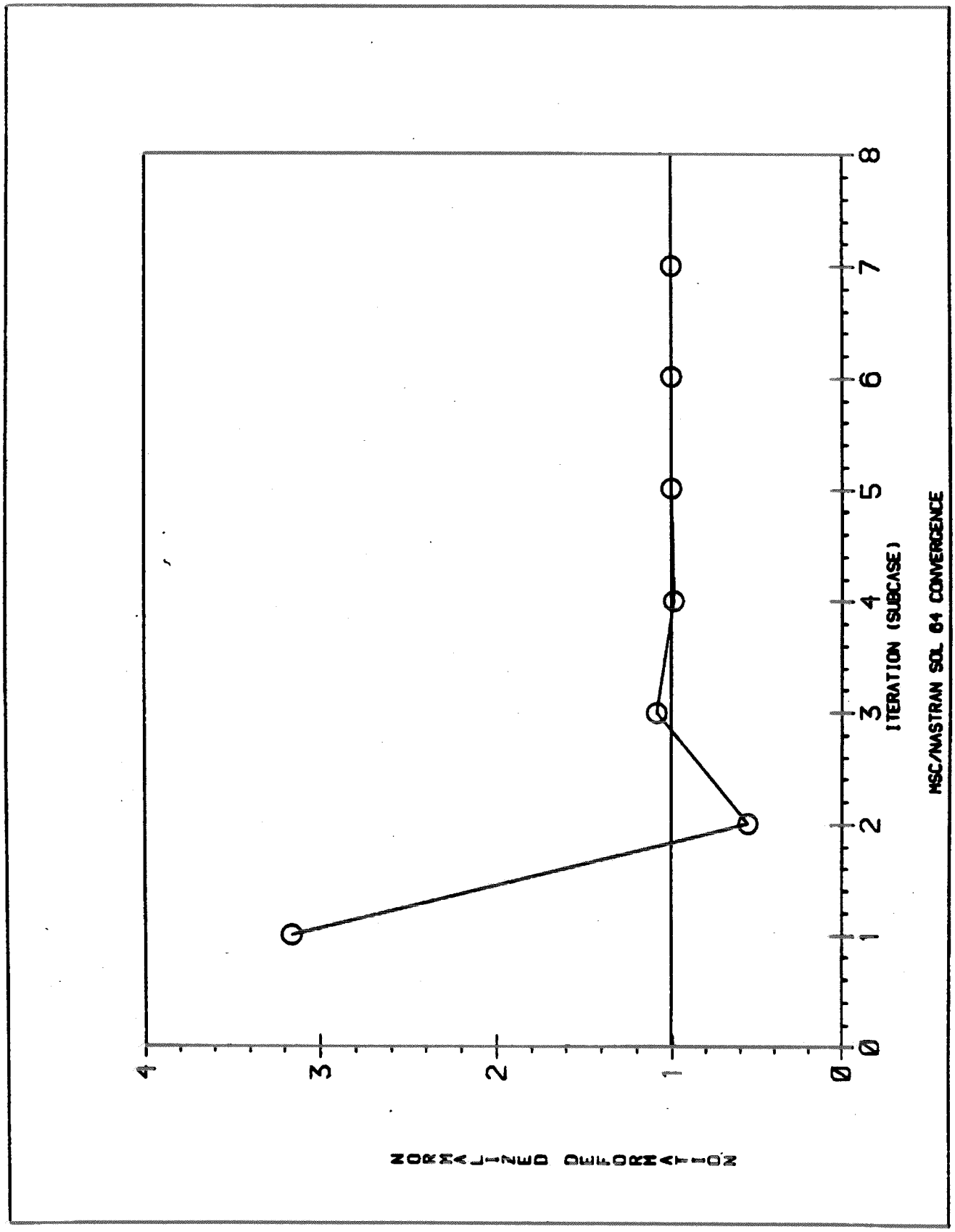

FIGURE 4. CONVERGENCE OF MSC/NASTRAN GEOMETRIC NON-LINEAR ANALYSIS OF MOTOR CASE

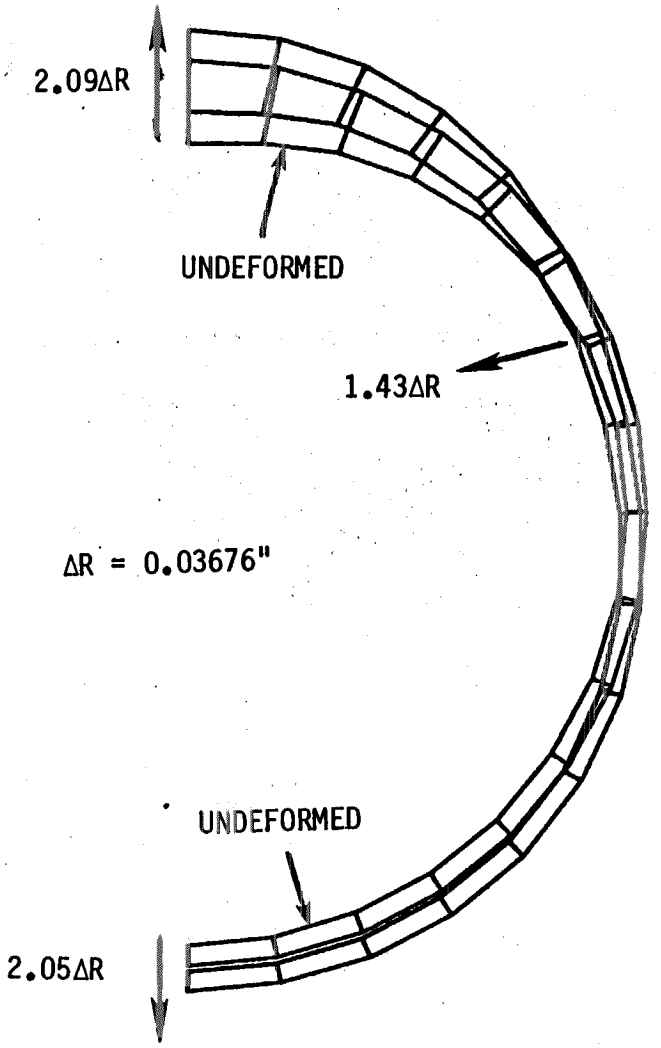

a) Longitudinal Plane of Symmetry

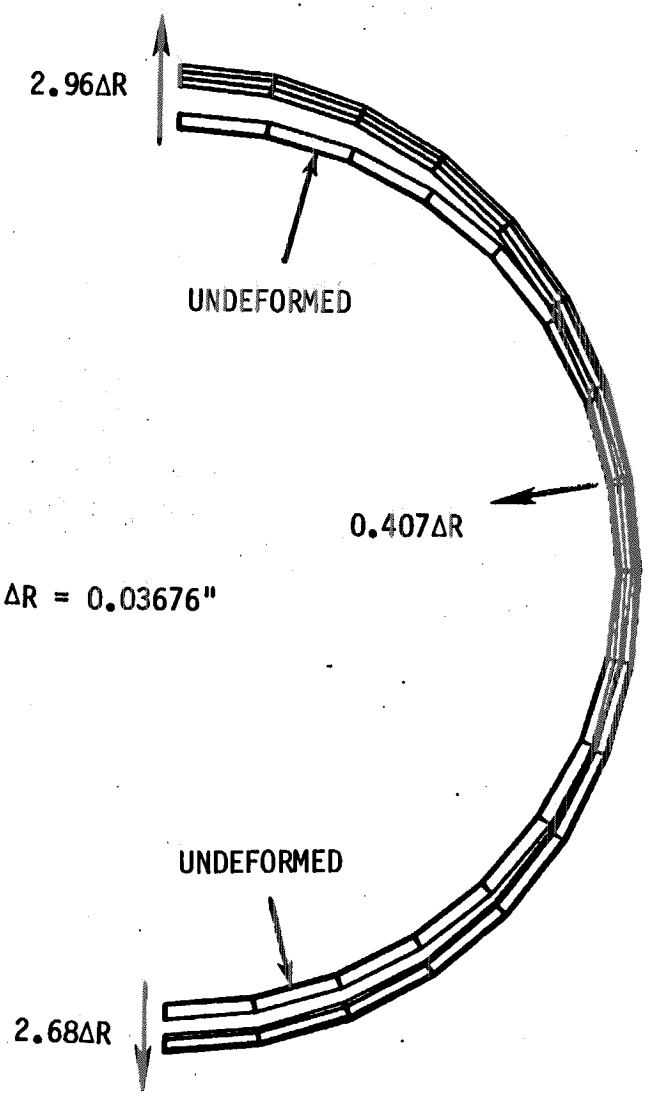

b) Free End

FIGURE 5. DEFORMED SHAPE OF MOTOR CASE (SOLID ELEMENT MODEL)

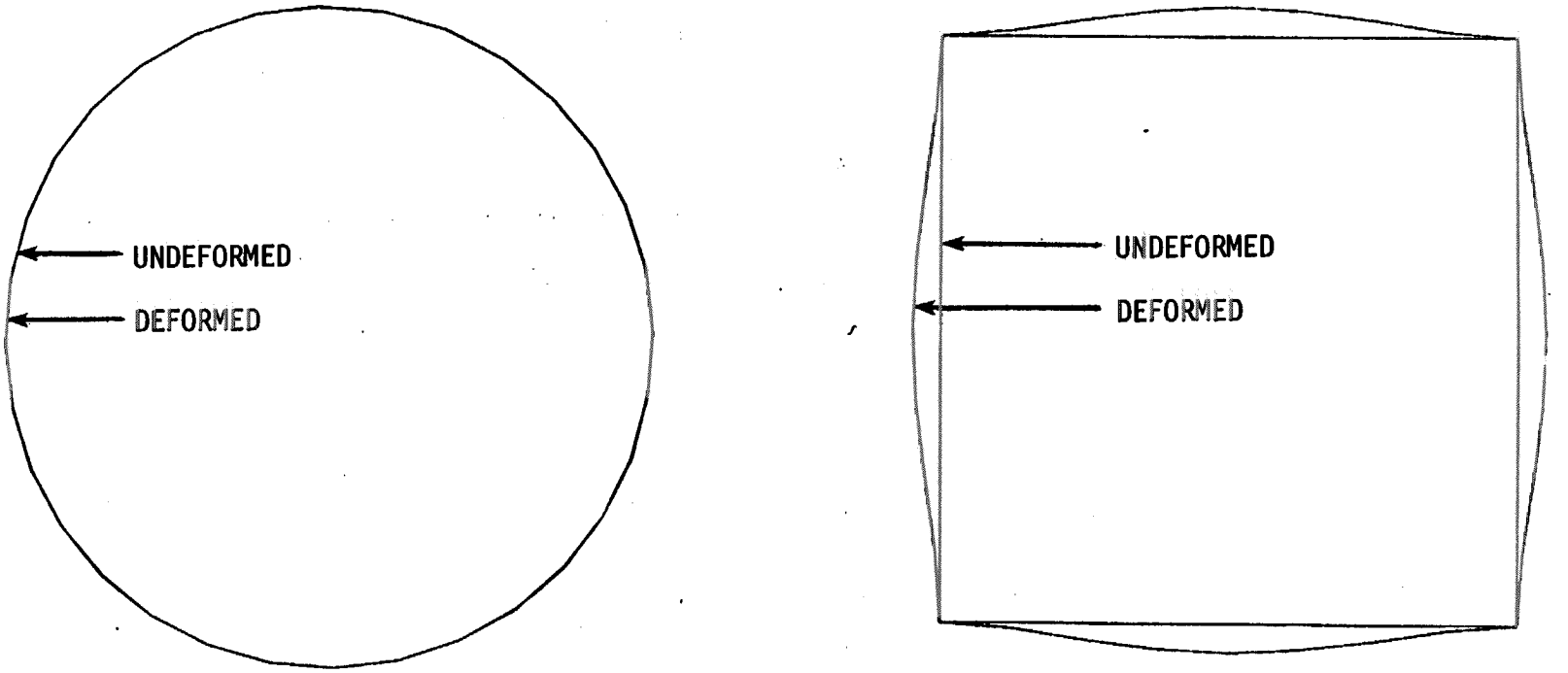

a) Circular Cross Section

b) Square Cross Section

FIGURE 6. DEFORMATION OF CIRCULAR AND SQUARE CROSS SECTIONS UNDER PRESSURE LOADING

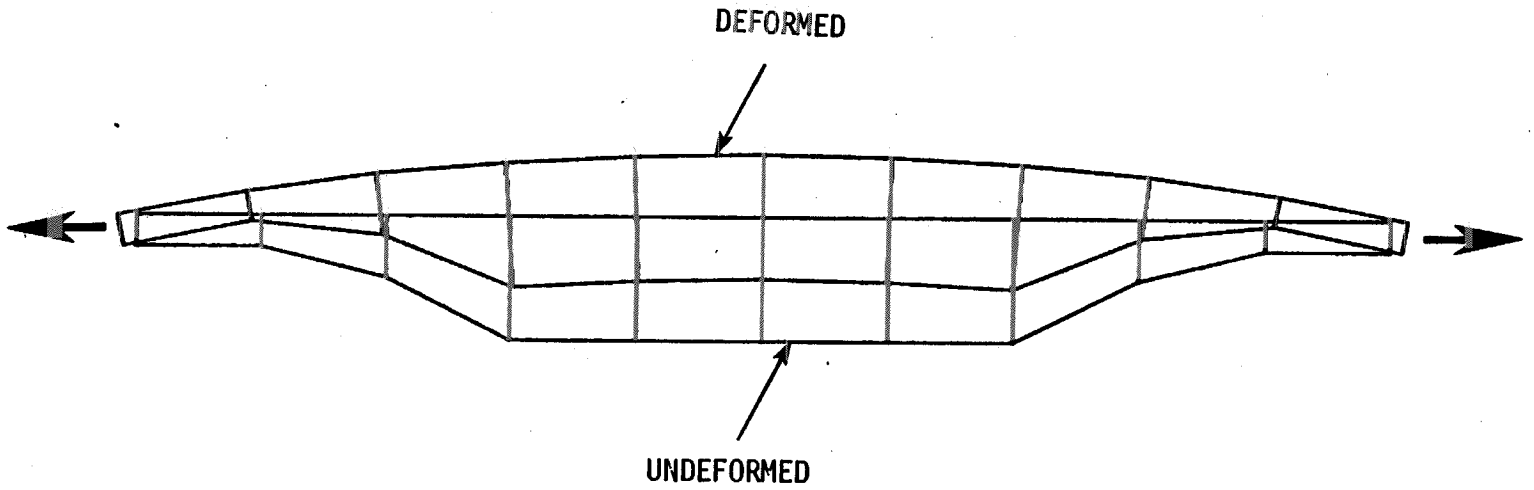

FIGURE 7. DEFORMATION OF ECCENTRICALLY LOADED BEAM

NOTE:

Grid Points are
Located at the
Mid-Shell thickness.

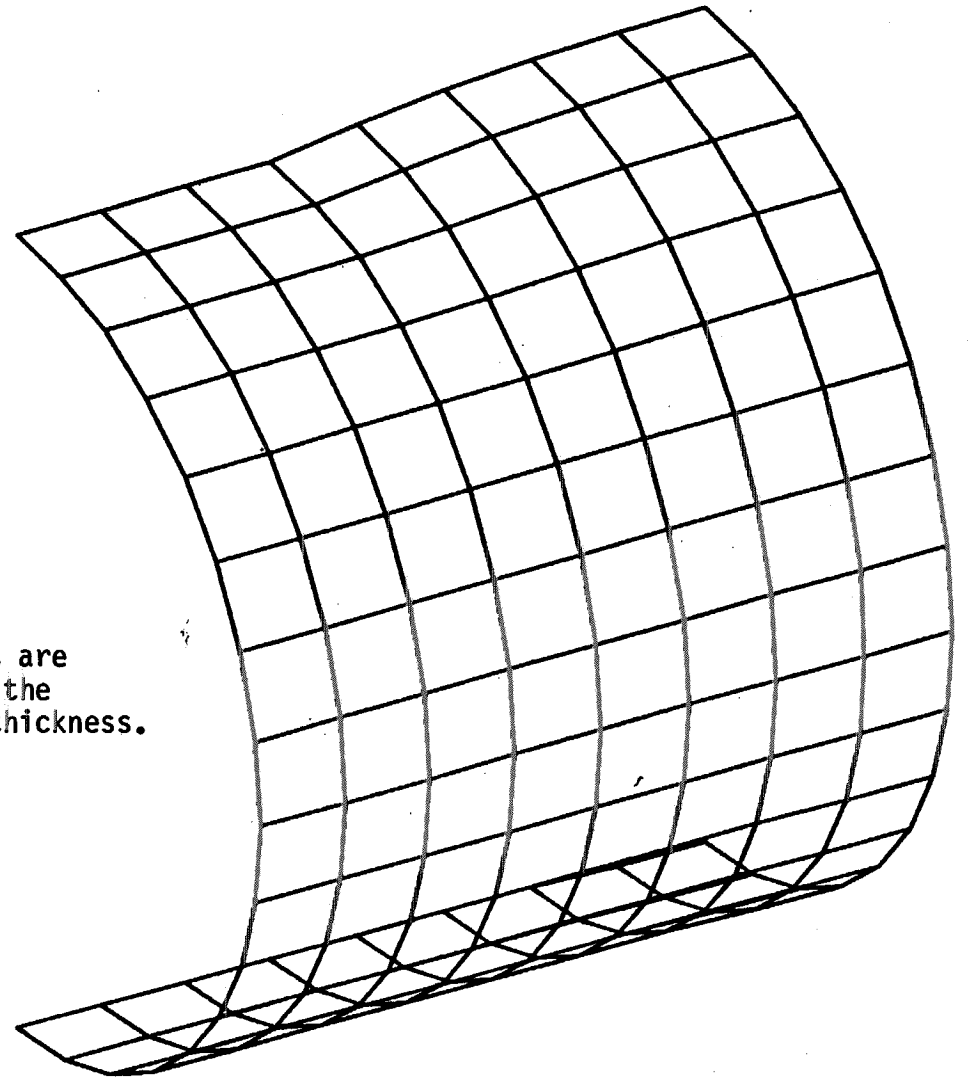

FIGURE 8. NASTRAN PLATE ELEMENT MODEL WITH VARIABLE RADIAL GEOMETRY AND VARIABLE SHELL THICKNESS

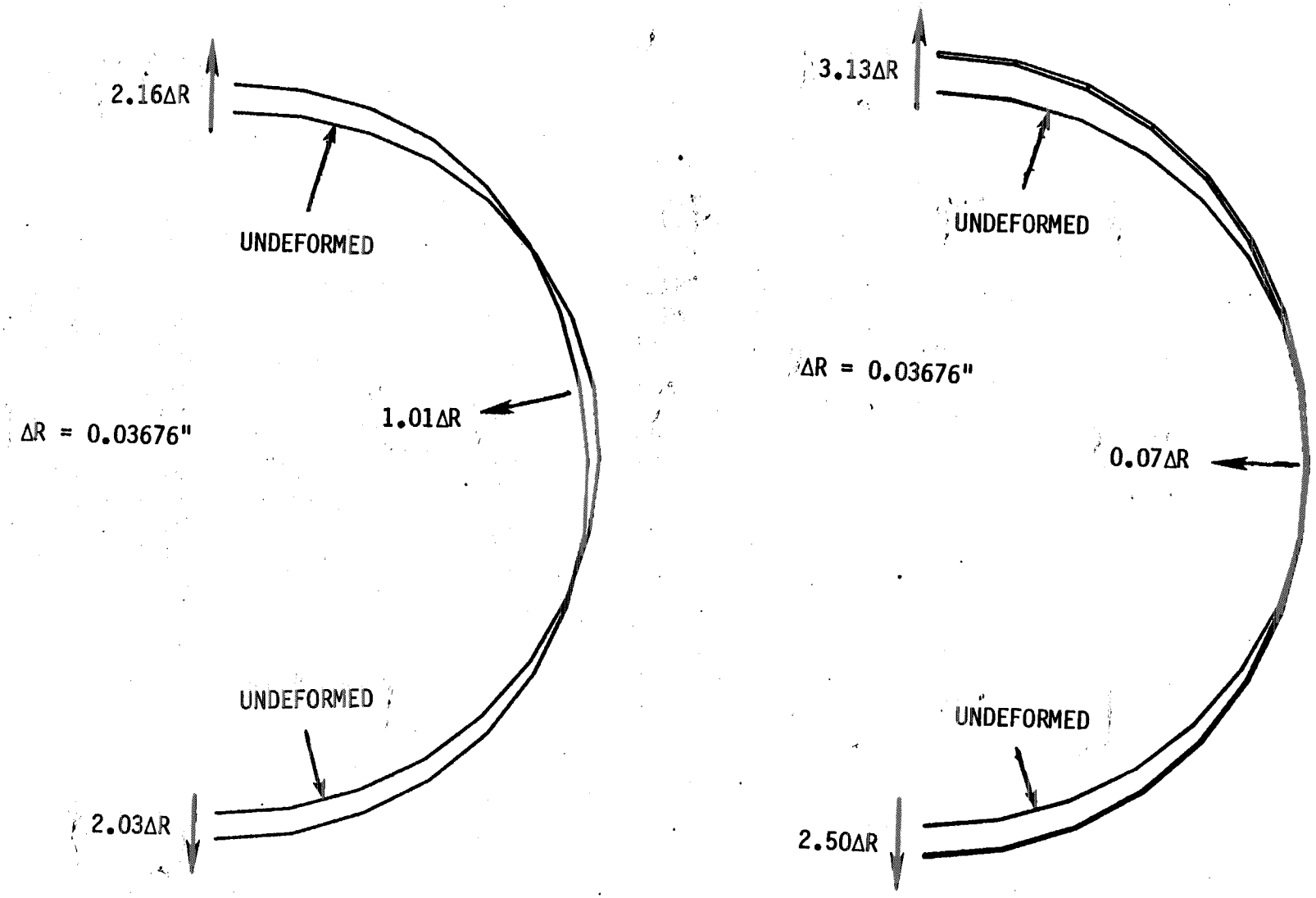

a) Longitudinal Plane of Symmetry

b) Free End

FIGURE 9. DEFORMED SHAPE OF MOTOR CASE PLATE ELEMENT MODEL WITH GRID POINTS AT MID-SHELL THICKNESS.

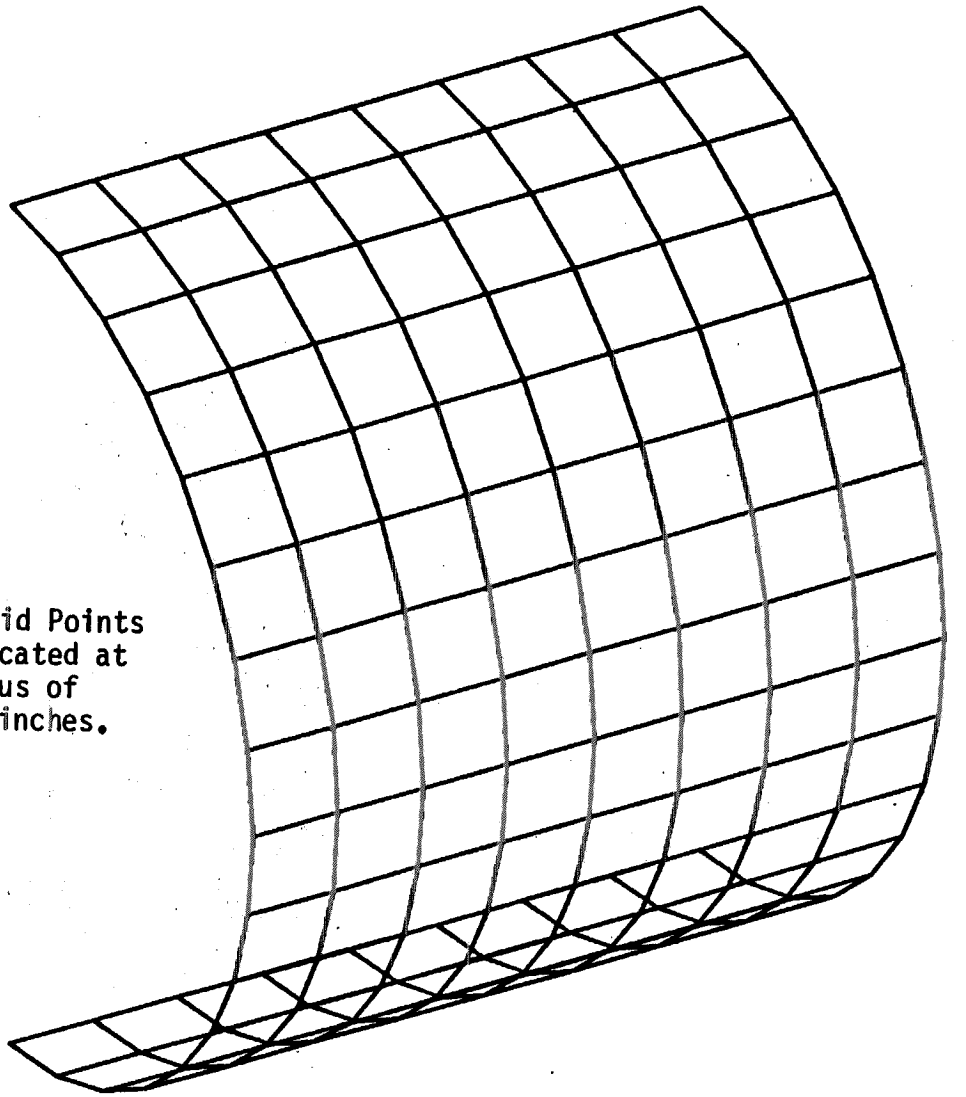

FIGURE 10. NASTRAN PLATE ELEMENT MODEL WITH CONSTANT RADIAL GEOMETRY AND VARIABLE SHELL THICKNESS

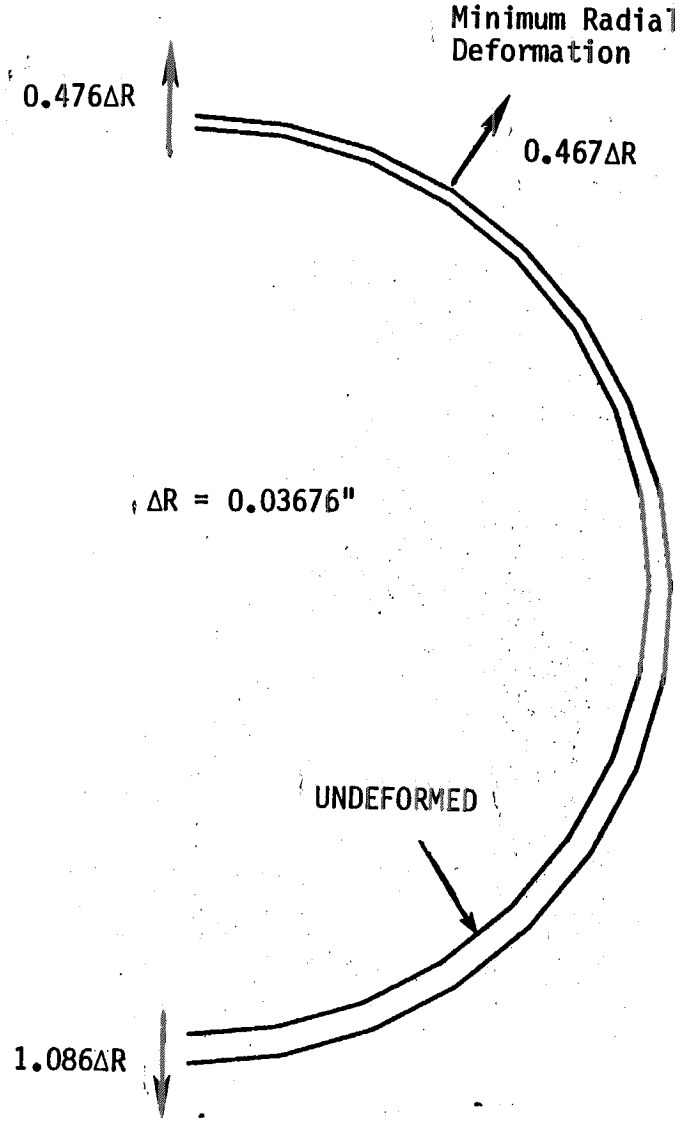

a) Longitudinal Plane of Symmetry

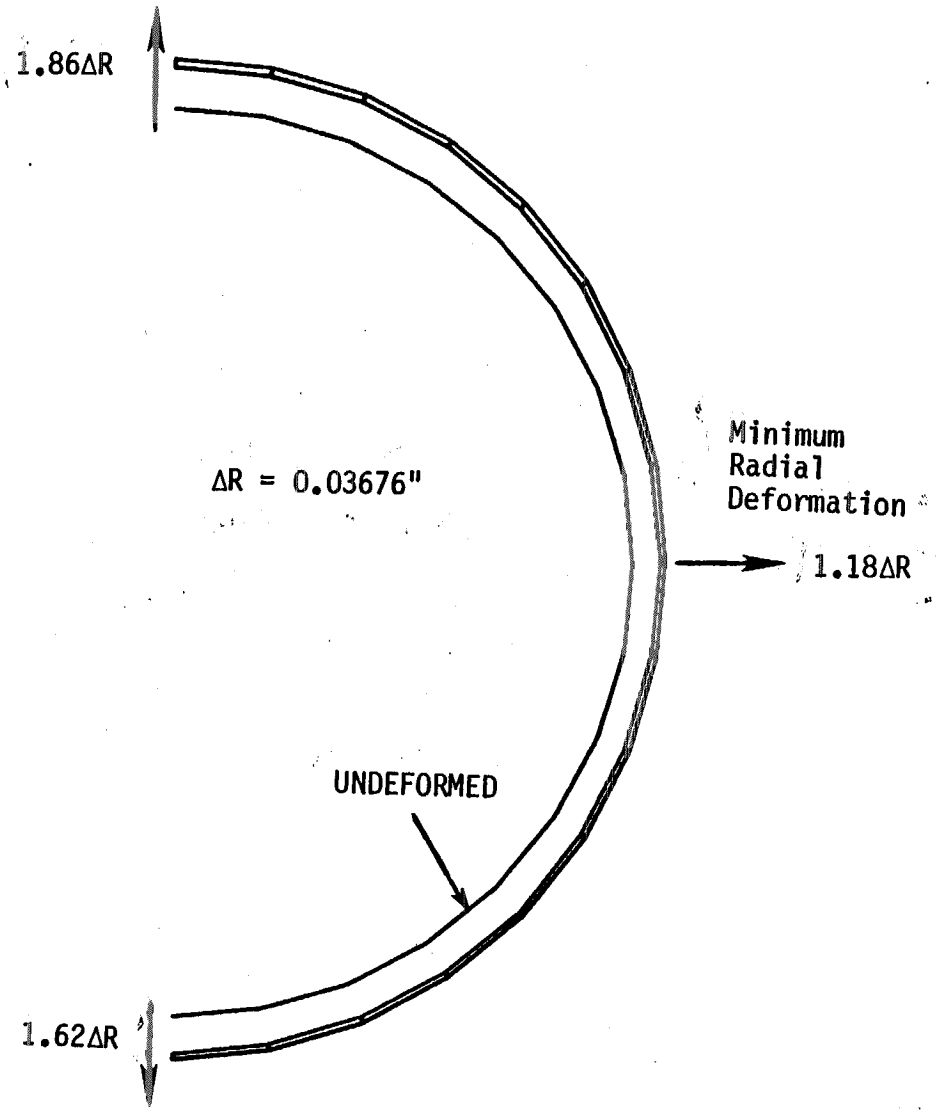

b) Free End

FIGURE 11. DEFORMED SHAPE OF MOTOR CASE PLATE ELEMENT MODEL WITH CONSTANT RADIAL GEOMETRY

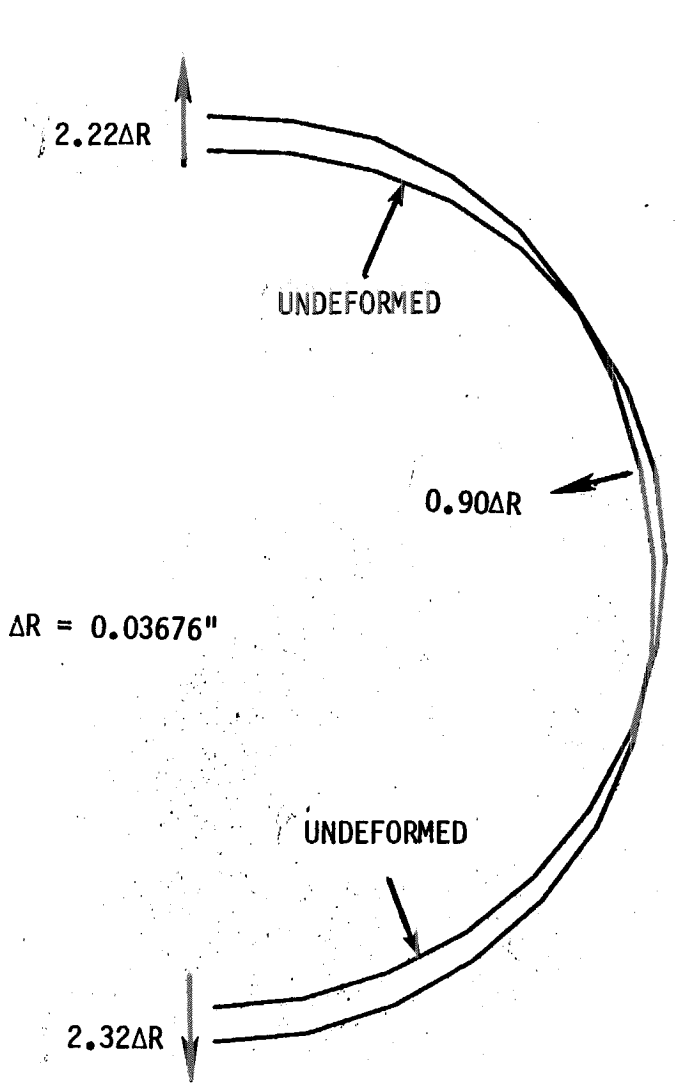

a) Longitudinal Plane of Symmetry

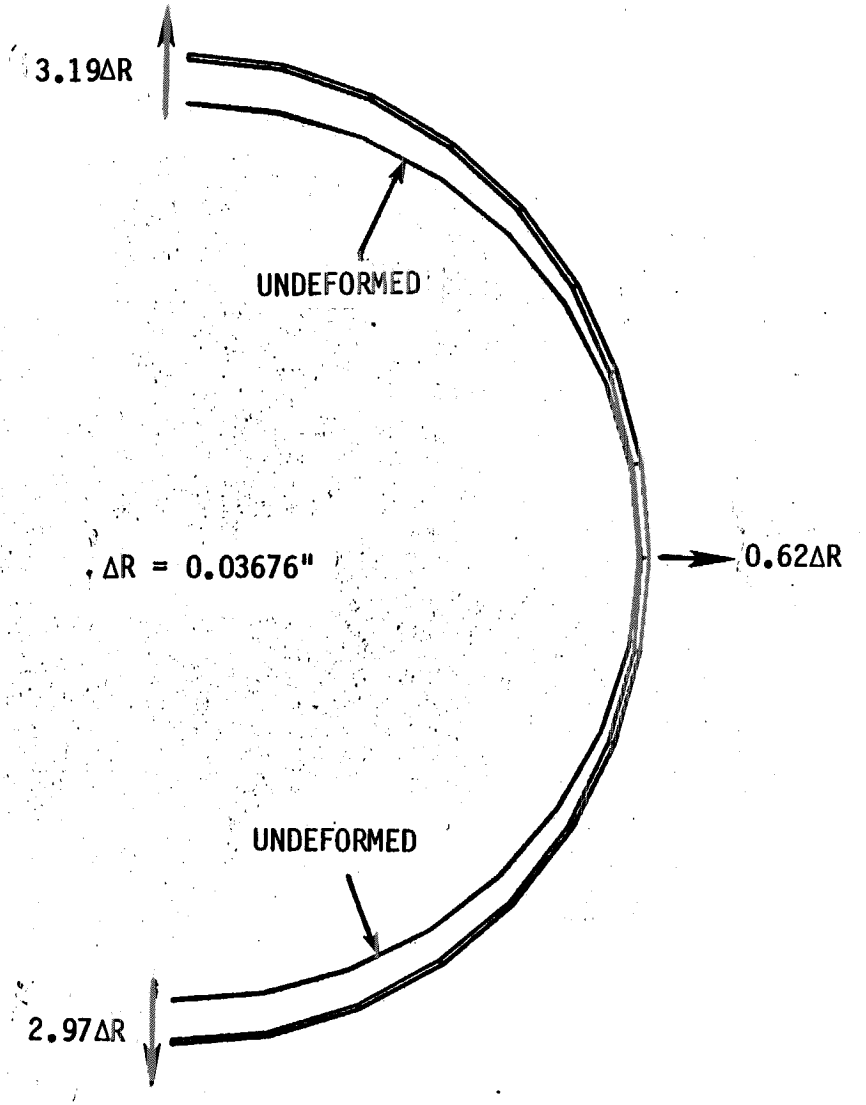

b) Free End

FIGURE 12. DEFORMED SHAPE OF MOTOR CASE PLATE ELEMENT MODEL WITHOUT LONGITUDINAL LOADS

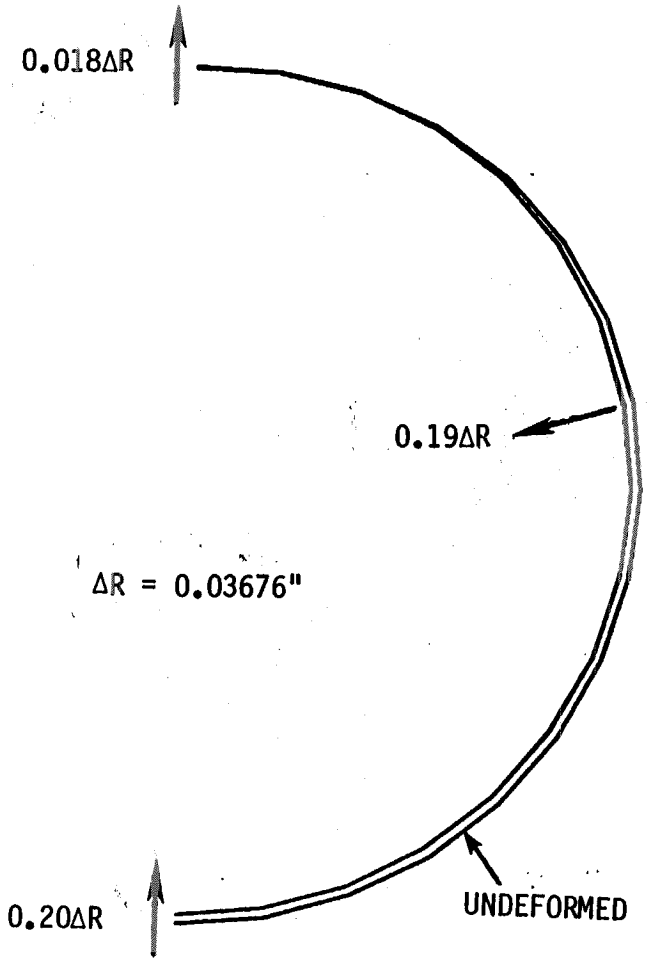

a) Longitudinal Plane of Symmetry

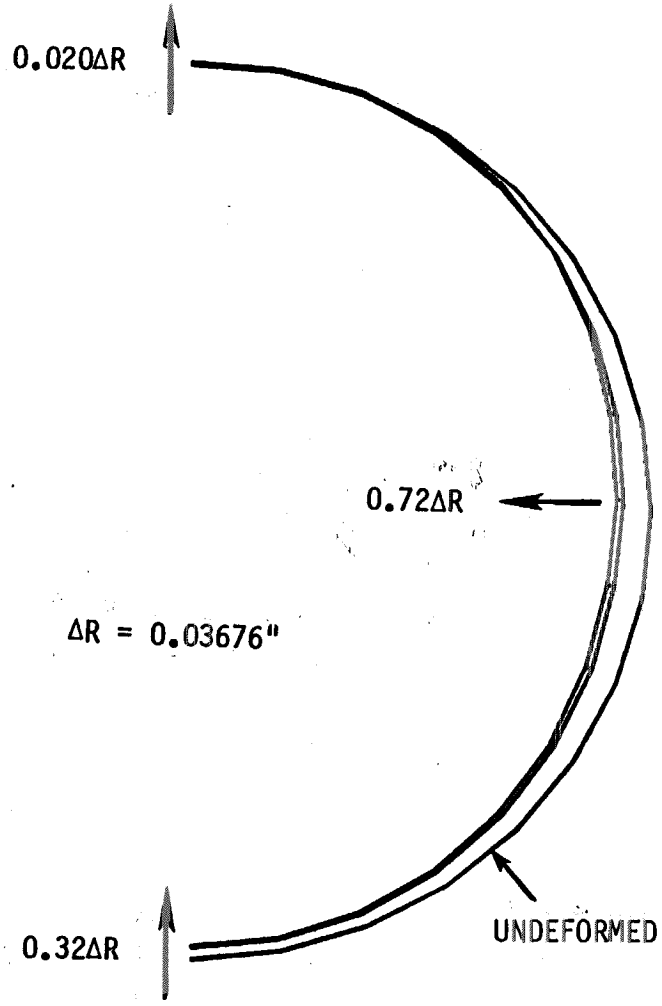

b) Free End

FIGURE 13. DEFORMED SHAPE OF MOTOR CASE PLATE ELEMENT MODEL WITH LONGITUDINAL LOADS ONLY

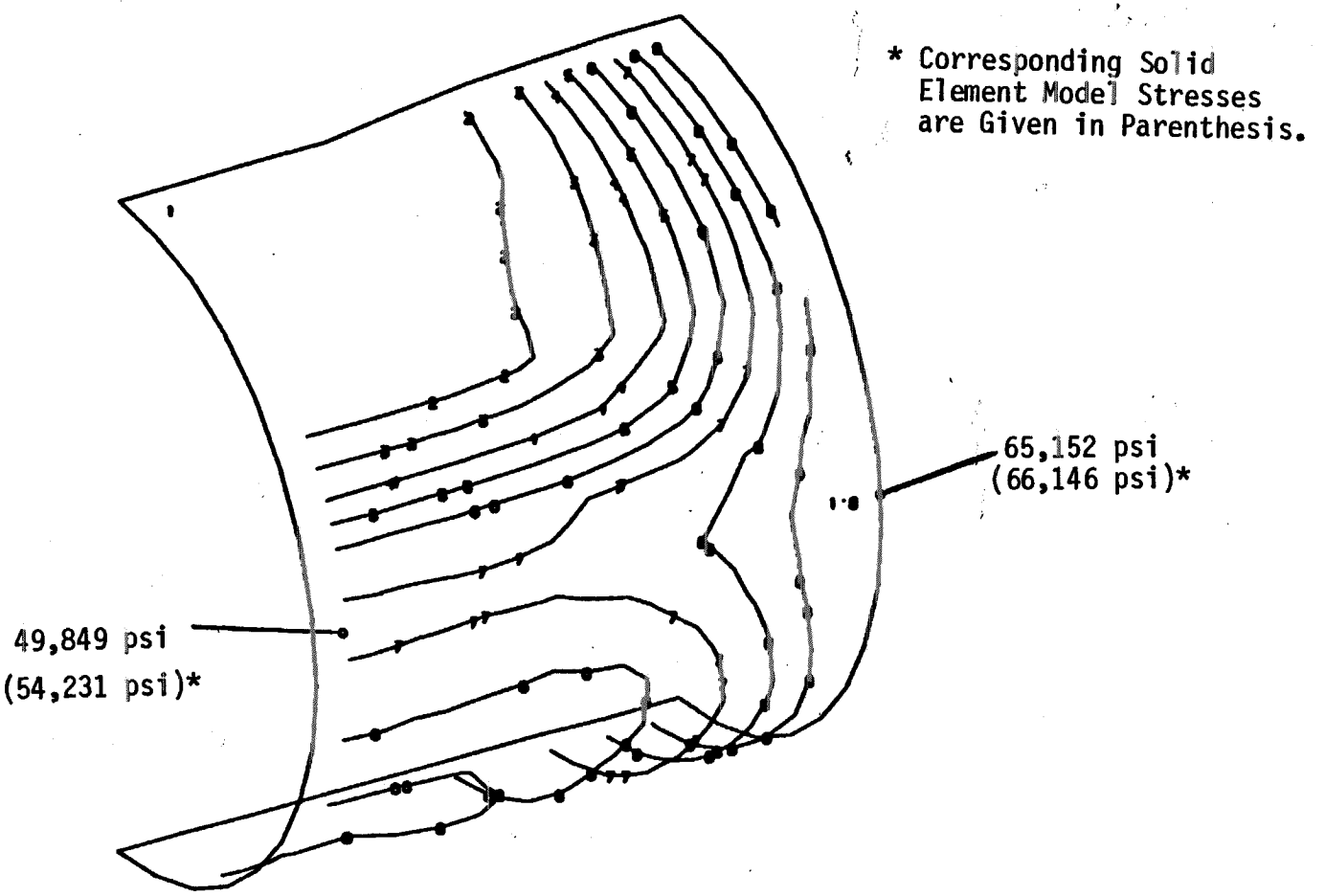

FIGURE 14. STRESS CONTOUR PLOT OF MOTOR CASE PLATE ELEMENT MODEL